



Performance-Based Optimization and Seismic Collapse Assessment of Self-Centering Steel Moment Frames with SMA-Based Connections

Aydin Hassanzadeh¹ and Saber Moradi^{2*}

¹PhD Candidate, Department of Civil Engineering, Toronto Metropolitan University, Toronto, ON, Canada

²Associate Professor, Department of Civil Engineering, Toronto Metropolitan University, Toronto, ON, Canada

*s.moradi@torontomu.ca (Corresponding Author)

ABSTRACT

This paper develops a performance-based seismic design optimization procedure for steel moment frames with shape memory alloy (SMA) connections. Considering the high cost of SMAs, the optimization study addresses the need for minimizing the use of SMA in low-damage building structures. A center of mass optimization algorithm is implemented for the design optimization of steel moment frames with SMA connections. The design variables are the cross-sectional area of beams and columns and the properties of SMA-based connections. The practical, strength-related, strong-column-and-weak-beam, and performance-based design constraints are defined in the optimization process. The initial relative cost of frames is regarded as the objective function. The developed performance-based design optimization methodology is demonstrated by optimizing three- and nine-story steel moment frames with SMA-based connections. Additionally, incremental dynamic analyses (IDAs) are performed to assess the seismic capacity of optimal steel moment frames with SMA connections. The collapse capacity of the optimal frames is assessed by generating IDA and fragility curves according to the FEMA P695 methodology and calculating adjusted collapse margin ratio (ACMR) values. Moreover, a trial-and-error design procedure is used to design non-optimal steel moment frames with SMA connections to provide the basis for comparisons and assessing the efficiency of the performance-based design optimization methodology. The seismic performance of optimal frames with SMA-based connections is compared with non-optimal frames in terms of initial relative cost, residual deformation, and seismic safety. The utilized methodology reduces the initial cost of the three- and nine-story frames by 4% and 13%, respectively. The residual story drifts for optimal and non-optimal frames are less than 0.5%. Moreover, optimal frames possess acceptable seismic safety.

Keywords: Shape memory alloy, Self-centering, Steel moment frame, Optimization, Performance-based design, Incremental dynamic analysis.

INTRODUCTION

During the past two decades, self-centering systems have been developed as an alternative to conventional seismic-resistant systems to prevent (or control) large residual deformation following a destructive earthquake. Shape memory alloys (SMAs) possess a distinctive shape recovery capability, which allows a building or bridge structure to return to its original upright position after unloading. As a result, these advanced materials have been increasingly utilized to mitigate seismic damage in civil engineering structures [1].

In the aftermath of the 1994 Northridge and 1995 Kobe earthquakes, fracture was observed in the welds joining the flange to the column of steel moment-resisting frames. Integrated SMA-steel connection is a vital alternative to conventional steel connections. Ocel et al. [2] proposed a connection consisting of four SMA bars connecting the beam flange to the column flange to reduce large residual deformation. These novel connections efficiently lower peak deformations and control residual deformations [3–5]. Furthermore, sensitivity analysis has been utilized to determine the most influential design parameters in these novel connections [6]. Moreover, surrogate models have been proposed to evaluate the response of SMA-based connections [7]. Performance-based design methodologies should be implemented to design optimal SMA-based moment frames.

Performance-based design methodologies lead to the designing of civil structures and infrastructures with reliable and predictable nonlinear structural performance. However, there appears to be a gap in implementing performance-based design

methodologies into the seismic design of steel moment-resisting frames with SMA-based connections. The performance-based design methodology has been utilized to design steel frames with SMA-based braces [8].

Optimization methodologies are powerful tools to automate the optimal design process of seismic systems. However, a few studies using optimization methodologies to design expensive SMA-based civil structures have been performed. Ozbulut [9] developed a genetic algorithm for reducing the structural response of a three-story steel frame with SMA-based braces. In [10], a performance-based design optimization methodology has been implemented to make a trade-off between safety and economics in SMA-braced frames.

Incremental dynamic analysis (IDA) [11] can be utilized to evaluate the collapse safety of the optimally designed structures. Previous studies evaluated the collapse capacity of concentrically braced frames by determining a collapse margin ratio (CMR) [12]. Some previous studies [10,13] have used IDA to study the seismic response of self-centering structures.

This study presents a performance-based design optimization of steel moment frames with SMA connections. The center of mass optimization algorithm [12,14] is utilized to find the optimal columns, beams, and SMA connections in the performance-based design context. In the optimization process, the initial cost of frames is considered the objective function. Four constraints are considered, including practical, strength-related, performance-based design, and strong-column-and-weak-beam checks. OpenSees [15] is utilized to develop numerical models in the optimization process. An artificial neural network model [16] is implemented to predict the responses of the SMA connections. Moreover, MATLAB [17] is implemented to code the optimization algorithm and post-processing tasks.

NUMERICAL MODELLING AND VERIFICATION

In OpenSees, "nonlinearBeamColumn" elements and "steel01" material are utilized to model beams and columns. The yield strength, modulus of elasticity, shear modulus, and strain hardening, respectively, are taken as 344.74 MPa, 200 GPa, 79.3 GPa, and 3%. In order to consider the second-order P-Delta effects in the numerical models, "P-Delta" transformation object available in the library of OpenSees is utilized. In this work, the effect of panel zones is not considered.

The SMA connection is modeled as a rotational spring using a "zeroLength" element. The "zeroLength" element is applied to connect the same coordinate nodes at the joint of beams and columns. The behavior of SMA connections is modeled by implementing "SelfCentering", "Pinching4", and "Steel01" materials in parallel.

A verification study is conducted to assess the accuracy of the implemented SMA connection models [18]. The coefficients for the linear combination of "SelfCentering", "Pinching4", and "Steel01" materials, respectively, are 0.90, 0.05, and 0.05. The accuracy of the utilized numerical model is compared with experimentally tested SMA connections, including SMA-D10-240d and SMA-D10-290 [18]. It is shown that the accuracy of the implemented numerical model is acceptable (Figure 1).

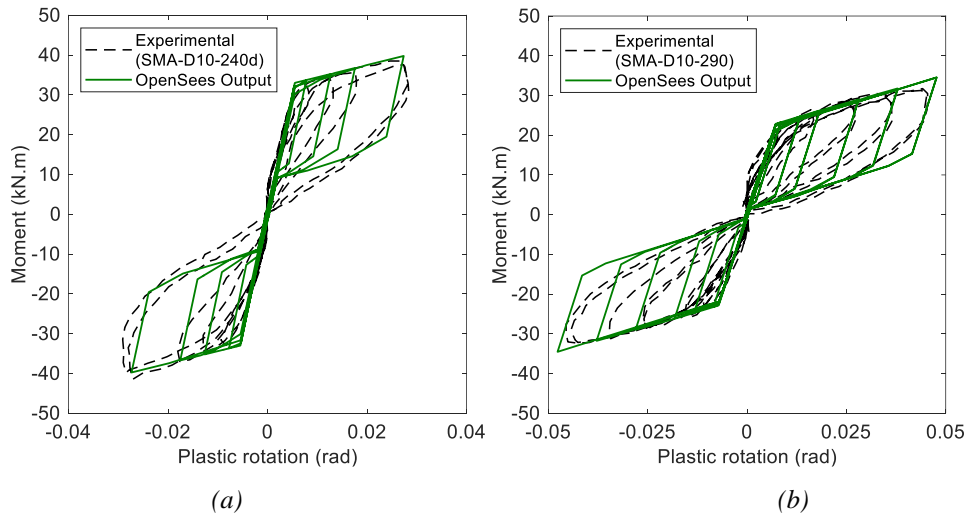


Figure 1. Verification: numerical vs. experimental results for specimens: (a) SMA-D10-240d (b) SMA-D10-290 [18].

In the optimization process, the moment-rotation backbone responses of the extended endplate connections with SMA bolts are predicted using artificial neural networks (ANN) trained by Nia and Moradi [16]. The trained ANNs are used to predict the moment-rotation backbone response parameters of SMA connections, including θ_B , θ_C , θ_E , M_B , M_C , M_E , and β as shown in Figure 2. Ten influential factors on the nonlinear behavior of the SMA connections are considered as the input variables of the trained ANNs [16]. These influential factors include martensite start stress, σ_{Ms} , martensite finish stress, σ_{Mf} , austenite start

stress, σ_{As} , austenite finish stress, σ_{Af} , maximum transformation strain, ε_L , SMA bolt pretension strain ratio, ε_{pt} , SMA bolt length, SB_L , SMA bolt diameter, SB_{dia} , beam depth, B_{dep} , and beam length, L_{beam} . NiTi SMA material properties, which are the first five influential parameters on the cyclic behavior of the utilized smart connections are reported in Table 1. E_{SMA} is the modulus of elasticity of SMA material.

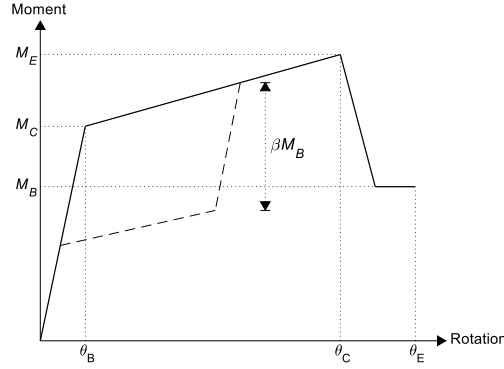


Figure 2. The idealized behavior curve for endplate connections with SMA bolts [16].

Table 1. Material properties for NiTi SMA bolts.

σ_{Ms} (MPa)	σ_{Mf} (MPa)	σ_{As} (MPa)	σ_{Af} (MPa)	E_{SMA} (GPa)
380	490	220	120	50

In addition to NiTi properties, the length of the beam is taken as 3 meters. Furthermore, the other influential parameters, including ε_{pt} , SB_L , SB_{dia} , and B_{dep} are optimization design variables. The ranges for these design variables, which are selected based on the practical constraints, are presented in Table 2. Moreover, the beam depth is selected based on the selected beam cross-section in the optimization process.

Table 2. Ranges for influential design variables.

	Symbol	Min	Max
Bolt pretension strain	ε_{pt}	0.005	0.015
Bolt length (mm)	SB_L	190	350
Bolt diameter (mm)	SB_{dia}	10	25

PERFORMANCE-BASED DESIGN OPTIMIZATION

This work uses a performance-based design optimization methodology for the seismic optimally design of SMA steel moment-resisting frames using a meta-heuristic algorithm, the center of mass optimization (CMO) [14]. Based on the physical concept of a center of mass, this meta-heuristic algorithm reduces the distance between particles with larger masses to the center of mass and vice versa. Reference [14] provides additional information. In the optimization process, the initial cost of steel moment frames with SMA connections is considered the objective function. Practical, strength-related, performance-based design and strong-column-and-weak-beam constraints are considered during the optimization process.

Performance-based design

In the performance-based seismic design context, two seismic performance levels, including immediate occupancy (IO) and collapse prevention (CP), are considered according to ASCE 41-17 [19]. The IO and CP performance levels correspond to 50% and 2% probability of exceedance in 50 years. To reduce the computational time of the optimization process, a nonlinear static analysis is implemented to assess the nonlinear structural responses of the frames in optimization. Additionally, the target displacement for the nonlinear static analysis is determined using Eq. (1). Furthermore, the first mode shape of the structures is considered to define the lateral loading in nonlinear static analysis.

$$\delta_t = C_0 C_1 C_2 S_a \frac{T_e^2}{4\pi^2} g \quad (1)$$

where C_0 , C_1 , and C_2 are the modification factors, which are defined according to ASCE 41-17 [19]; T_e is the effective fundamental period of the structure; S_a is the response spectrum acceleration at T_e , which is determined in accordance with ASCE 7-22 [20]; and g is the acceleration of gravity.

Design variables

In the performance-based design optimization of steel moment frames with SMA connections, the cross-section of columns and beams and properties of SMA bolts are considered as design variables as follows:

$$X = \begin{cases} X_C = \{C_1, C_2, \dots, C_{nc}\} \\ X_B = \{B_1, B_2, \dots, B_{nb}\} \\ X_{SP} = \{SP_1, SP_2, \dots, SP_{ncg}\} \\ X_{SL} = \{SL_1, SL_2, \dots, SL_{ncg}\} \\ X_{SD} = \{SD_1, SD_2, \dots, SD_{ncg}\} \end{cases} \quad (2)$$

where X_C , X_B , X_{SP} , X_{SL} , and X_{SD} , respectively, are the column, beam, SMA bolt pretension strain, SMA bolt length, and SMA bolt diameter design variable vectors; nc , nb , ncg are the number of columns, beams, connection properties groups.

The selected structural sections for beams and columns are designated as highly ductile members, which are reported in Table 3. The SMA bolt length ranges from 190 mm to 350 mm, the cross-section diameter ranges from 10 mm to 25 mm, and the pretension strain ranges from 0.005 to 0.015.

Table 3. Selected sections for beams and columns

Columns		Beams	
W14×455	W14×193	W24×76	W21×50
W14×426	W14×176	W21×73	W18×50
W14×398	W14×159	W21×68	W16×50
W14×370	W14×145	W21×62	W18×46
W14×342	W14×132	W24×62	W16×45
W14×311	W14×82	W18×60	W21×44
W14×283	W14×74	W21×57	W18×40
W14×257	W14×68	W16×57	W16×40
W14×233	W14×53	W24×55	W18×35
W14×211	W14×48	W18×55	

Initial cost

The initial relative cost of structural members and SMA-based connections, respectively denoted as C_S and C_{SM} , can be determined using Eq. (3).

$$C_l = C_S + C_{SM} \quad (3)$$

$$C_l = \sum_{i=1}^{n_{st}} \rho_i A_i L_i C'_s / C'_s + \sum_{j=1}^{n_{sm}} 8 \times \rho_j A_j L_j C'_{sm} / C'_{st}$$

$$C_l = \sum_{i=1}^{n_{ste}} \rho_i A_i L_i + \sum_{j=1}^{n_{smb}} 8 \times \rho_j A_j L_j C_r$$

where C'_s and C'_{sm} are the cost of steel and SMA material per unit weight, respectively; C_r is the ratio of C'_s to C'_{sm} . C_r is taken as 1 and 100 for steel structural elements and SMA bolts [21], respectively. ρ_i and ρ_j are, respectively, the weight density for steel elements and SMA bolts; A_i and A_j are the cross-sectional area for steel beams and columns and SMA bolts; L_i and L_j are the length of steel members and SMA bolts, respectively; n_{st} and n_{sm} are respectively the numbers of columns and beams and SMA connections. Furthermore, the initial relative cost of SMA connections is multiplied by eight due to the existence of eight SMA bolts in the utilized connections, as written in Eq. (3).

Problem formulation

In the optimization process, the initial relative cost of steel moment frames with SMA connections is considered the objective function. Practical, g_P , strength-related, g_S , performance-based design, g_{PBD} , strong-column-and-weak-beam, g_{SCWB} , constraints are considered during the optimization process. The optimization problem can be formulated as follows:

Find design variable vectors: X

To minimize: $C_l(X)$ (4)

$$\text{Subject to: } \begin{cases} g_P \leq 0 \\ g_S \leq 0 \\ g_{PBD} \leq 0 \\ g_{SCWB} \leq 0 \end{cases}$$

Constraints

The practical constraints must be satisfied at beam-to-column and column-to-column joints, as given in Eq. (5):

$$g_{P,i} = \begin{cases} g_{P1,i}(X) = \frac{Be_i^f}{Co_i^f} - 1 \leq 0 \\ g_{P2,i}(X) = \frac{Co_i^{f,u}}{Co_i^{f,l}} - 1 \leq 0 \\ g_{P3,i}(X) = \frac{Co_i^{d,u}}{Co_i^{d,l}} - 1 \leq 0 \\ g_{P4,i}(X) = \frac{Co_i^{t,u}}{Co_i^{t,l}} - 1 \leq 0 \end{cases}, \quad i = 1, 2, \dots, n_j \quad (5)$$

where Be_i^f and Co_i^f are respectively the flange width of the beams and columns connected to the i th joint; $Co_i^{f,u}$ and $Co_i^{f,l}$ are respectively the flange width of upper and lower columns; $Co_i^{d,u}$ and $Co_i^{d,l}$ are respectively the depth of upper and lower columns; $Co_i^{t,u}$ and $Co_i^{t,l}$ are respectively the web thickness of the upper and lower columns; and n_j is the number of joints.

The strength-related constraints are checked for structural members, including columns and beams, assuming that frames with SMA connections are special steel moment frames to reduce the design space. In this regard, the equivalent lateral force (ELF) procedure is implemented to check the strength-related constraints [20].

The strength-related constraints are checked by performing the ELF procedure following AISC 360-16 [22] as follows:

$$g_{S,j} = \begin{cases} g_{GS1,j}(X) = \frac{P_{rj}}{P_{c,j}} + \frac{8}{9} \frac{M_{rj}}{M_{c,j}} - 1 \leq 0, \text{ if } \frac{P_{rj}}{P_{c,j}} \geq 0.2 \\ g_{GS2,j}(X) = \frac{1}{2} \frac{P_{rj}}{P_{c,j}} + \frac{M_{rj}}{M_{c,j}} - 1 \leq 0, \text{ if } \frac{P_{rj}}{P_{c,j}} < 0.2 \end{cases}, \quad j = 1, 2, \dots, n_{se} \quad (6)$$

where P_r and M_r are respectively the required axial and flexural strengths; P_c and M_c are respectively the design axial and flexural strengths, which are determined according to Chapters E and F in AISC 360-16 [22]; and n_{se} is the total number of beams and columns.

Following the practical and strength-related constraints, the performance-based design checks, including story drifts, columns and beams behavior, and rotation of SMA connection, are defined.

The story drift checks are considered as follows:

$$g_{\Delta}(X) = \frac{\Delta_{pl}}{\Delta_{all,pl}} - 1 \leq 0 \quad (7)$$

where Δ_{pl} and $\Delta_{per,pl}$, respectively, are the story drifts and permissible story drift at the IO and CP performance levels; and $\Delta_{per,IO}$ and $\Delta_{per,CP}$, respectively, are taken as 0.7% and 5%.

The categorization of columns into deformation-controlled (DC) or force-controlled (FC) depends on the P_G/P_{ye} ratio, where P_G is the axial force component under gravity load, and P_{ye} is the expected axial yield capacity. If the P_G/P_{ye} ratio is below 0.6, the column falls into the DC category. For DC columns, the limitations on rotation can be specified as follows:

$$g_{DC,k}(X) = \frac{\theta_{C,k}^{pl}}{\theta_{C,k}^{per,pl}} - 1 \leq 0, \quad k = 1, 2, \dots, n_{dc} \quad (8)$$

where $\theta_{C,k}^{pl}$ and $\theta_{C,k}^{per,pl}$, respectively, are the maximum absolute plastic rotations and permissible plastic rotation at pl performance levels for the k th column; and n_{dc} is the total number of the DC columns. In order to ensure that columns remain elastic after destructive earthquakes, the allowable rotation for columns at all the performance levels is yield rotation [19].

If the P_G/P_{ye} ratio is 0.6 or greater, the column will be classified as FC. The FC columns must adhere to the following limitations:

$$g_{FC,l} = \begin{cases} g_{FC1,l}(X) = \frac{P_{u,l}^{pl}}{P_{yLB,l}} + \frac{8}{9} \frac{M_{u,l}^{pl}}{M_{plB,l}} - 1 \leq 0, \text{ if } \frac{P_{u,l}^{pl}}{P_{yLB,l}} \geq 0.2 \\ g_{FC2,l}(X) = \frac{1}{2} \frac{P_{u,l}^{pl}}{P_{yLB,l}} + \frac{M_{u,l}^{pl}}{M_{plB,l}} - 1 \leq 0, \text{ if } \frac{P_{u,l}^{pl}}{P_{yLB,l}} < 0.2 \end{cases}, \quad l = 1, 2, \dots, n_{fc} \quad (9)$$

where $P_{u,l}^{pl}$ and $M_{u,l}^{pl}$, respectively, represent the axial force and moment at each performance level; and $P_{yLB,l}$ and $M_{pLB,l}$, respectively, indicate the lower-bound axial yield and moment capacity of the l th column. and n_{fc} is the total number of the FC columns.

The rotation constraints for beams can be written as follows:

$$g_{B,n}(X) = \frac{\theta_{B,n}^{pl}}{\theta_{B,n}^{per,pl}} - 1 \leq 0, n = 1, 2, \dots, n_b \quad (10)$$

where $\theta_{Be,n}^{pl}$ and $\theta_{Be,n}^{per,pl}$, respectively, are the maximum absolute rotation and permissible plastic rotation of the n th beam at pl performance level; and n_b is the number of beams. In order to ensure that beam remain elastic after severe earthquakes, the permissible rotation for beams at all the performance levels is yield rotation [19].

The constraint for SMA connections is written as follows:

$$g_{SMA,o}(X) = \frac{\theta_{SMA,o}^{pl}}{\theta_{SMA,o}^{all,pl}} - 1 \leq 0, o = 1, 2, \dots, n_{SMA} \quad (11)$$

where $\theta_{SMA,o}^{pl}$ is the o th connection rotation each performance level; $\theta_{SMA,o}^{per,pl}$ is the permissible rotation of SMA connections, which is determined using trained ANNs [16]. The permissible rotation of SMA connections at IO and CP performance levels are θ_B and θ_C (Figure 2).

The strong-column-and-weak-beam constraint is checked in accordance with AISC 341-16 [23] using Eq. (12).

$$g_{SCWB}(X) = \frac{\sum M_{pb}}{\sum M_{pc}} - 1 < 0 \quad (12)$$

where M_{pb} and M_{pc} are, respectively, the flexural strength of beams and columns at each joint.

COLLAPSE ASSESSMENT

The seismic safety of optimal steel moment frames with SMA connections is evaluated by determining collapse margin ratio (CMR) values following an efficient procedure reported in FEMA P695 [24]. To conduct IDA, a suit of 22 ground motions incrementally scaled to the maximum considered earthquake (MCE) intensity level, reported in Table 4, is chosen. In addition, IDA plots are generated to capture the engineering demand parameters (EDPs) for various intensity measures (IMs). The EDPs for the optimal designs are recorded as the maximum story drifts and the 5% damped spectral acceleration at the fundamental period, which are used as the IMs. In this work, the collapse criteria are considered as follows: (1) the peak story drift exceeds 10%, (2) the nonlinear time-history analysis fails to converge.

The CMR is determined as follows:

$$CMR = \frac{IM_{50\%}}{IM_{MCE}} \quad (13)$$

where $IM_{50\%}$ and IM_{MCE} are the spectral acceleration for which 50% of selected earthquake ground motions result in collapse and the 5% damped spectral acceleration at the MCE level.

The adjusted collapse margin ratio ($ACMR$) is calculated using Eq. (14) to take into account the spectral shape effect, which is considered by using the spectral shape factor (SSF). The SSF is calculated according to Table 7-1 of FEMA P695.

$$ACMR = SSF \times CMR \quad (14)$$

The acceptable $ACMR$ is determined considering different sources of uncertainty, including the record-to-record variability of the collapse data, β_{RTR} , the design requirements, β_{DR} , test data, β_{TD} , and modeling, β_{MDL} . The β_{RTR} is computed using Equation (7-2) of FEMA P695. Furthermore, β_{DR} , β_{TD} , and β_{MDL} are taken as 0.1, 0.2, and 0.2, respectively. Total collapse uncertainty, β_{TOT} , is calculated as follows:

$$\beta_{TOT} = \sqrt{\beta_{RTR}^2 + \beta_{DR}^2 + \beta_{TD}^2 + \beta_{MDL}^2} \quad (15)$$

Using Eq. (16), the $ACMR$ values of optimal designs are compared to an acceptable $ACMR_{20\%}$ (Table 7-3 of FEMA P69).

$$ACMR \geq ACMR_{20\%} \quad (16)$$

Table 4. Ground motion record sets.

No.	Earthquake			Recording Station	Record Motion	
	M	Year	Name		PGA _{max} (g)	PGV _{max} (cm/s.)
1	6.7	1994	Northridge	Beverly Hills - Mulhol	0.52	63
2	6.7	1994	Northridge	Canyon Country-WLC	0.48	45
3	7.1	1999	Duzce, Turkey	Bolu	0.82	62
4	7.1	1999	Hector Mine	Hector	0.34	42
5	6.5	1979	Imperial Valley	Delta	0.35	33
6	6.5	1979	Imperial Valley	El Centro Array #11	0.38	42
7	6.9	1995	Kobe, Japan	Nishi-Akashi	0.51	37
8	6.9	1995	Kobe, Japan	Shin-Osaka	0.24	38
9	7.5	1999	Kocaeli, Turkey	Duzce	0.36	59
10	7.5	1999	Kocaeli, Turkey	Arcelik	0.22	40
11	7.3	1992	Landers	Yermo Fire Station	0.24	52
12	7.3	1992	Landers	Coolwater	0.42	42
13	6.9	1989	Loma Prieta	Capitola	0.53	35
14	6.9	1989	Loma Prieta	Gilroy Array #3	0.56	45
15	7.4	1990	Manjil, Iran	Abbar	0.51	54
16	6.5	1987	Superstition Hills	El Centro Imp. Co.	0.36	46
17	6.5	1987	Superstition Hills	Poe Road (temp)	0.45	36
18	7.0	1992	Cape Mendocino	Rio Dell Overpass	0.55	44
19	7.6	1999	Chi-Chi, Taiwan	CHY101	0.44	115
20	7.6	1999	Chi-Chi, Taiwan	TCU045	0.51	39
21	6.6	1971	San Fernando	LA - Hollywood Stor	0.21	19
22	6.5	1976	Friuli, Italy	Tolmezzo	0.35	31

OPTIMIZATION AND COLLAPSE ASSESSMENT RESULTS

This section presents the optimization and seismic assessment results. The initial relative cost optimization methodology is implemented to design 3-story and 9-story steel moment frames with SMA connections in the performance-based design context. Figure 3 presents 3- and 9-story frames and the grouping of structural members. In addition, the grouping of SMA connection properties is the same as the grouping of beams.

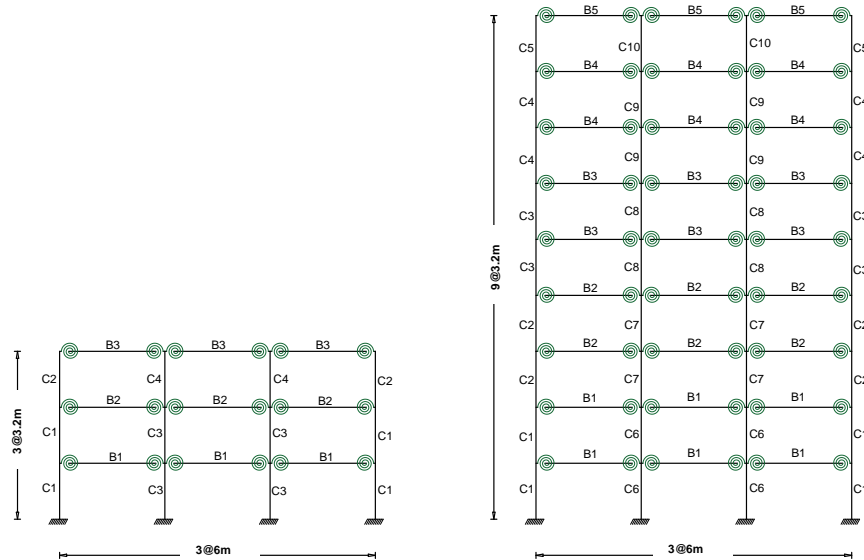


Figure 3. Grouping details of structural elements for 3- and 9-story frames.

In order to provide readers with a deeper understanding of the efficiency of the proposed performance-based design initial relative cost optimization methodology, a trial-and-error procedure is utilized to design one steel moment frame with SMA connections in the framework of performance-based.

Results for 3-Story frames

The CMO algorithm is implemented to optimize the 3-story steel moment frames with SMA connections in the performance-based design framework. The optimization and trial-and-error design results are reported in Table 5. The optimal and non-optimal 3-story frames are denoted by OSMRF3st and NSMRF3st, respectively. It is observed that the initial relative cost of OSMRF3st is 4% lesser.

Table 5. Performance-based design results for 3-story frames

	OSMRF3st	NSMRF3st
C1	W14×68	W14×48
C2	W14×48	W14×48
C3	W14×82	W14×132
C4	W14×68	W14×48
B1	W21×44	W18×35
B2	W18×35	W16×45
B3	W18×35	W18×35
$\epsilon_{pt,1}$ (%)	1	1
$\epsilon_{pt,2}$ (%)	1	1
$\epsilon_{pt,3}$ (%)	1	1
SB _{L,1} (mm)	190	190
SB _{L,2} (mm)	190	190
SB _{L,3} (mm)	190	190
SB _{dia,1} (mm)	16	16
SB _{dia,2} (mm)	16	16
SB _{dia,3} (mm)	14	14
C_I	10295	10677

C: Column; B: Beam; ϵ_{pt} : SMA Bolt Prestrain; SB_L: SMA Bolt Length; SB_{dia}: SMA Bolt Diameter; C_I : Initial Relative Cost

The story and residual drifts comparison of 3-story frames are presented in Figure 4. It is observed that optimal and non-optimal 3-story steel moment frames with SMA connections have similar performance in terms of story and residual story drifts. The residual drifts for optimal and non-optimal steel moment frames with SMA connections are less than 0.5%, which shows that using performance-based design methodology and SMA connections results in economically repairable frames.

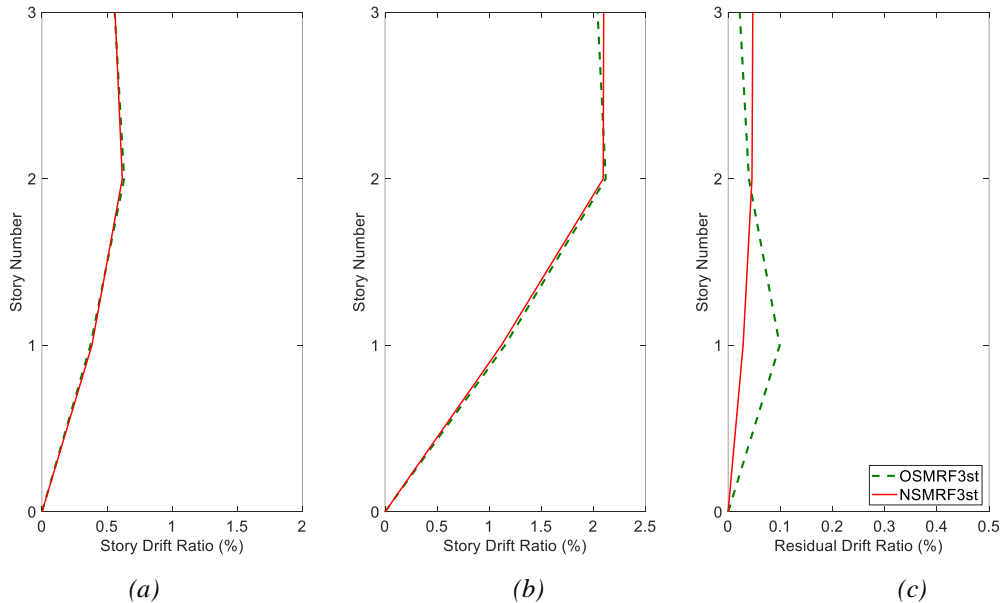


Figure 4. Story drift distribution for 3-story frames at (a) IO; (b) CP performance levels; and (c) residual story drift ratio under MCE level.

The seismic assessment results for 3-story structures are reported in Table 6. It is shown that both optimal and non-optimal 3-story frames have the same *ACMR* values and are of acceptable seismic safety. It is shown that using the presented performance-based design optimization methodology results in acceptable collapse safety.

Table 6. Collapse assessment results for 3-story frames

	<i>CMR</i>	<i>SSF</i>	<i>ACMR</i>	<i>ACMR</i> _{20%}	Pass/Fail
OSMRF3st	2.04	1.20	2.45	1.51	P
NSMRF3st	2.03	1.20	2.44	1.51	P

Results for 9-Story frames

For 9-story frames, the prestraining for the 9-story frames is taken 0.008, which is the same as the SMA transformation start strain. The seismic optimization methodology is implemented to design steel moment frames with SMA connections in the performance-based design context. The optimization and trial-and-error design results are reported in Table 7. The optimal and non-optimal 9-story frames are denoted by OSMRF9st and NSMRF9st, respectively. It is observed that the initial relative cost of OSMRF9st is 13% lesser.

Table 7. Performance-based design results for 9-story frames

	OSMRF9st	NSMRF9st
C1	W14×193	W14×132
C2	W14×145	W14×68
C3	W14×74	W14×68
C4	W14×48	W14×48
C5	W14×48	W14×48
C6	W14×193	W14×132
C7	W14×132	W14×132
C8	W14×132	W14×132
C9	W14×74	W14×68
C10	W14×48	W14×48
B1	W24×62	W24×55
B2	W24×55	W16×57
B3	W21×44	W16×57
B4	W18×35	W18×35
B5	W18×35	W18×35
SB _{L,1} (mm)	270	190
SB _{L,2} (mm)	190	190
SB _{L,3} (mm)	190	190
SB _{L,4} (mm)	190	190
SB _{L,5} (mm)	190	190
SB _{dia,1} (mm)	16	24
SB _{dia,2} (mm)	20	24
SB _{dia,3} (mm)	20	24
SB _{dia,4} (mm)	16	24
SB _{dia,5} (mm)	12	24
<i>C_I</i>	45053	51606

C: Column; B: Beam; SB_L: SMA Bolt Length; BD: SMA Bolt Diameter; *C_I*: Initial Relative Cost

The story and residual drifts comparison of 9-story frames are presented in Figure 5. Similar to 3-story frames, the residual story drifts for optimal and non-optimal 9-story designs are less than 0.5% due to considering performance-based design constraints and SMA connections.

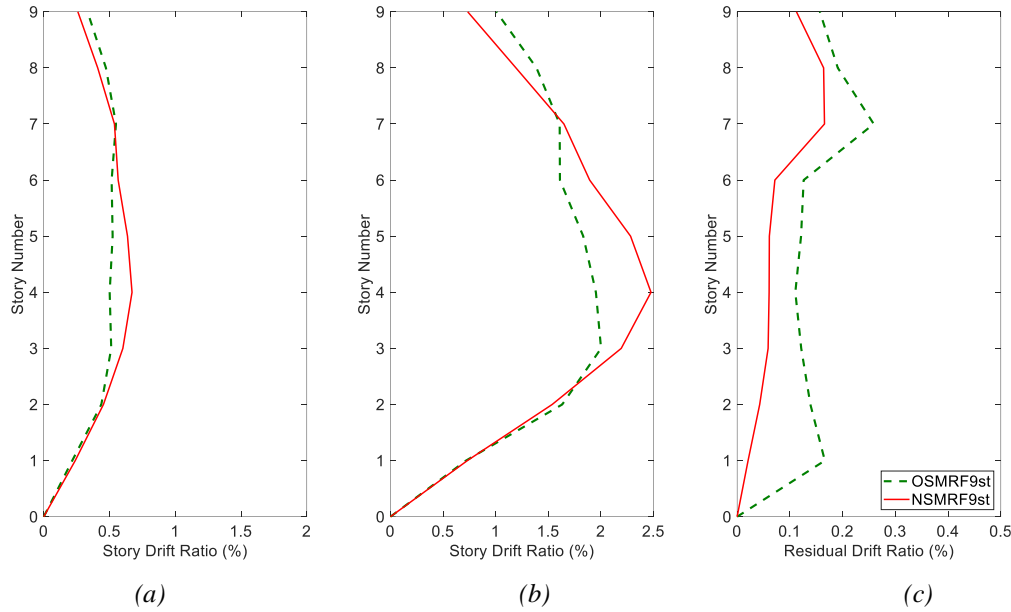


Figure 5. Story drift distribution for 9-story frames at (a) IO; (b) CP performance levels; and (c) residual story drift ratio under MCE level.

The seismic assessment results for 3-story structures are reported in Table 8. Similar to 3-story frames, the optimal and non-optimal 9-story frames are of acceptable and the same *ACMR* values.

Table 8. Collapse assessment results for 3-story frames

	<i>CMR</i>	<i>SSF</i>	<i>ACMR</i>	<i>ACMR</i> _{20%}	Pass/Fail
OSMRF9st	1.44	1.27	1.83	1.51	P
NSMRF9st	1.60	1.16	1.86	1.40	P

CONCLUSIONS

This study presents a performance-based design optimization methodology to design steel moment frames with shape memory alloy (SMA) connections. The main goal of this work is to minimize the initial relative cost of steel moment frames with SMA connections. During the optimization process, the initial relative cost of designs is considered the objective function. The cross-sectional area of beams and columns and the properties of SMA-based connections are considered design variables. Four different types of constraints, including practical, strength-related, performance-based design, and strong-column-and-weak-beam checks, are considered in the optimization. Furthermore, a trial-and-error design process is utilized to design non-optimal frames with SMA connections. Subsequently, the seismic safety of the optimal and non-optimal designs is assessed using the methodology in FEMA P695. Finally, the initial relative costs, story, residual story drifts, and seismic safety of the optimal and non-optimal designs are compared. The performance-based design optimization is performed on 3- and 9-story steel moment frames with SMA-based connections. The main results from this work is summarized as follows:

- The utilized performance-based design optimization methodology reduces the initial relative cost of steel moment frames with SMA connections. The initial relative costs for optimal 3- and 9-story frames are 4% and 13% less than those of non-optimal frames.
- For optimal and non-optimal 3- and 9-story frames, the residual story drifts are less than 0.5%, which shows that using performance-based design methodology and SMA connections results in economically repairable designs following severe earthquakes.
- For 3- and 9-story frames, optimal and non-optimal designs have the same *ACMR* values indicating acceptable collapse capacity.

Future research is recommended to reduce the total cost of steel moment frames considering damage indices in the optimization process. Furthermore, topology optimization methodologies can be utilized to efficiently reduce the initial cost of expensive SMA-based steel moment frames.

ACKNOWLEDGMENTS

The research presented in this paper was financially supported by the Toronto Metropolitan University Faculty of Engineering and Architectural Science, and the Natural Sciences and Engineering Research Council of Canada (NSERC) through Discovery Grant. The authors gratefully acknowledge the financial support.

REFERENCES

- [1] Auricchio, F., Fugazza, D., and DesRoches, R. (2006). "Earthquake performance of steel frames with nitinol braces." *Journal of Earthquake Engineering*,10:45–66.
- [2] Ocel, J., Desroches, R., Leon, RT., Gregory Hess, W., Krumme, R., et al. (2004). "Steel beam-column connections using shape memory alloys." *Journal of Structural Engineering*, 130:732–40.
- [3] Taftali B. (2007). "Probabilistic seismic demand assessment of steel frames with shape memory alloy connections." Georgia Institute of Technology.
- [4] DesRoches, R., Taftali, B., and Ellingwood, BR. (2010). "Seismic performance assessment of steel frames with shape memory alloy connections. Part I—analysis and seismic demands." *Journal of Earthquake Engineering*,14:471–86.
- [5] Ellingwood, BR., Taftali, B., and DesRoches, R. (2010). "Seismic performance assessment of steel frames with shape memory alloy connections, Part II—Probabilistic seismic demand assessment." *Journal of Earthquake Engineering*, 14:631–45.
- [6] Nia, MM., and Moradi, S. (2020). "Limit state behavior and response sensitivity analysis of endplate steel connections with shape memory alloy bolts." *Journal of Intelligent Material Systems and Structures*, 31:2071–87.
- [7] Nia, MM., and Moradi, S. (2021). "Surrogate models for endplate beam-column connections with shape memory alloy bolts." *Journal of Constructional Steel Research*, 187:106929.
- [8] Qiu, C-X., and Zhu, S. (2017). "Performance-based seismic design of self-centering steel frames with SMA-based braces." *Engineering Structures*, 130:67–82.
- [9] Ozbulut, OE., Roschke, PN., Lin, PY., and Loh, CH. (2010). "GA-based optimum design of a shape memory alloy device for seismic response mitigation." *Smart Materials and Structures*, 19:065004.
- [10] Hassanzadeh, A., and Moradi, S. (2022). "Topology optimization and seismic collapse assessment of shape memory alloy (SMA)-braced frames: effectiveness of Fe-based SMAs." *Frontiers of Structural and Civil Engineering*, 2022:1–21.
- [11] Vamvatsikos, D., and Cornell, CA. (2002). "Incremental dynamic analysis." *Earthquake Engineering & Structural Dynamics*, 31:491–514.
- [12] Hassanzadeh, A., and Gholizadeh, S. (2019). "Collapse-performance-aided design optimization of steel concentrically braced frames." *Engineering Structures*, 197.
- [13] Moradi, S., Alam, MS., and Asgarian, B. (2014). "Incremental dynamic analysis of steel frames equipped with NiTi shape memory alloy braces." *Structural Design of Tall and Special Buildings*, 23:1406–25.
- [14] Gholizadeh, S., Ebadijalal, M. (2018). "Performance based discrete topology optimization of steel braced frames by a new metaheuristic." *Advances in Engineering Software*, 123:77–92.
- [15] Mazzoni, S., McKenna, F., Scott, MH., Fenves, L., et al. (2013). OpenSees [Computer Software]: The Open System for Earthquake Engineering Simulation.
- [16] Nia, MM., and Moradi, S. (2022). "Artificial neural network-based predictive tool for modeling of self-centering endplate connections with SMA bolts." *Journal of Structural Engineering*, 148:4022198.
- [17] MATLAB. (2019). The language of technical computing.
- [18] Fang, C., Yam, MCH., Lam, ACC., and Xie, L. (2014). "Cyclic performance of extended end-plate connections equipped with shape memory alloy bolts." *Journal of Constructional Steel Research*, 94:122–36.
- [19] ASCE 41-17. (2017). Seismic evaluation and retrofit of existing buildings. Reston (VA): American Society of Civil Engineers.
- [20] ASCE 7. (2022) Minimum design loads and associated criteria for buildings and other structures. American Society of Civil Engineers.

- [21] Qiu, C., and Du, X. (2019). "Seismic performance of multistory CBFs with novel recentering energy dissipative braces." *Journal of Constructional Steel Research*, 105864.
- [22] ANSI/AISC 360-16. (2016). Specification for structural steel buildings. Chicago Illinois, USA: American Institute of Steel Construction.
- [23] AISC 341-16. (2016). Seismic provisions for structural steel buildings. Chicago Illinois, USA: American Institute of Steel Construction.
- [24] FEMA P695. (2009). Quantification of building seismic performance factors. Washington (DC): Federal Emergency Management Agency.